EARTHQUAKE ENGINEERING AND STRUCTURAL DYNAMICS, VOL. 14, 19-40 (1986)

SEISMIC SHEAR VIBRATION OF EMBANKMENT DAMS IN SEMI-CYLINDRICAL VALLEYS

PANOS DAKOULAS AND GEORGE GAZETAS

Department of Civil Engineering, Rensselaer Polytechnic Institute, Troy, N.Y. 12180, U.S.A.

SUMMARY

A rigorous analytical solution is developed for the lateral linear shear response of embankment dams in semi-cylindrical valleys. Closed-form algebraic expressions are presented pertaining to both free and base-induced oscillations, and extensive parametric and comparative studies elucidate the prominent effects of canyon geometry (shape and aspect ratio) on dynamic response. Harmonic steady-state as well as earthquake-induced accelerations, displacements and shear strains in the dam are studied and compared with those obtained from 3-Dimensional analyses for other canyon geometries, as well as from 2-Dimensional (2-D) analyses of the dam mid-section. It is shown that such 2-D analyses may provide significantly lower values of near-crest accelerations, but slightly higher values of shear strains and stresses than the 3-D analyses. The proposed method of analysis is at least three orders of magnitude less expensive than other presently available numerical procedures.

INTRODUCTION

About 30 years ago Hatanaka[1] and Ambraseys[2] showed that the fundamental natural frequency in lateral shear vibration of a dam built in a narrow rectangular canyon is higher than that of an infinitely long dam with an identical cross-section. These early studies were only isolated attempts to address the issue of the effects of canyon geometry (shape and dimensions) on the dynamic response of earth and rockfill dams. It is only in the last 5 years that satisfactory solutions have been developed to this complicated 3-Dimensional (3-D) problem.

Martinez and Bielak[3] studied the lateral response of earth structures having a plane of symmetry perpendicular to the longitudinal axis. To avoid the expense of 3-D finite-element analyses, they used a 2-D (plane) finite-element in conjunction with a Fourier expansion of the solution in the longitudinal direction; displacements and forces were considered to be the sum of the contribution of a limited set of modes. Longitudinal displacements were ignored and natural frequencies and shapes were obtained by solving the corresponding eigenvalue problem. The presented results showed substantial differences in response between dams in rectangular and triangular narrow canyons.

A different approximate formulation has been presented by Ohmachi.[4, 5] Both longitudinal and vertical displacements were ignored and the dam was divided into superelements through vertical, closely-spaced transverse planes. Thus, each element had the shape of a truncated pyramid, the bases of which were two neighbouring cross-sections. It was then assumed to behave during vibration as a triangular shear beam whose geometry and properties correspond to the middle section of that element. Thus, the law of distribution of displacements within each element was obtained from the shear-beam modal shapes. A linear interpolation function was used to express the displacement shape in the longitudinal direction and by enforcing compatibility of deformation between the superelements, the solution was obtained in the form of natural frequencies and modal shapes. Ohmachi's results for rectangular, trapezoidal and triangular canyons confirmed the significance of canyon geometry found by Martinez and Bielak,[3] although there are some quantitative differences in the natural frequencies reported in these two studies for dams in triangular canyons.

Makdisi *et al.*[6] developed a 3-D finite-element formulation by replacing the 2-D plane-strain isoparametric elements of the computer code LUSH by prismatic longitudinal elements with six faces and eight nodal points.

0098–8847/86/010019–22$02.20

Received 11 December 1984
Revised 19 April 1985

To reduce computer storage and time requirements, they ignored longitudinal displacements and assumed that only shear waves can propagate vertically and horizontally in the embankment. Using this model, results were obtained and presented for steady-state and transient response of homogeneous dams in triangular canyons. Subsequent work at Berkeley[7, 8] avoided the aforementioned simplifying restriction on longitudinal deformations and presented results for acceleration and shear stresses developed in an idealized and in an actual dam cross-section. These studies showed that the presence of the rigid triangular boundary increases the fundamental frequencies, and seems to increase the seismic accelerations while decreasing the seismic shear strains. More extensive parameter studies using this formulation would certainly be of interest.

Finally, Abdel-Ghaffar and Koh[9] developed a solution which is based on the Rayleigh–Ritz method, uses sinusoidal basis functions and involves an appropriate transformation of the dam geometry into a cuboid. Results have been presented for natural frequencies and mode shapes of a dam in a trapezoidal canyon.

Despite all this substantial progress, much has still to be learned regarding the factors influencing the seismic behaviour of embankment dams built in narrow valleys. Moreover, and in view of the very high computer storage and time requirements of most of the aforementioned formulations, it would be desirable to achieve closed-form analytical solutions for some idealized canyon geometries. Availability of such solutions would (i) allow extensive parameter studies to be conducted inexpensively, whence considerable insight could be gained into the dynamics of the problem; (ii) provide a means of checking the more sophisticated formulations; and (iii) offer a valuable tool for preliminary design calculations.

To this end, the present paper develops a closed-form analytical solution for the dynamic lateral response of an embankment dam built in a semi-cylindrical canyon, as sketched in Figure 1. Only linear shearing deformations are considered and the results are presented in the form of suprisingly simple algebraic expressions for natural frequencies, modal shapes, steady-state transfer functions for harmonic base motion

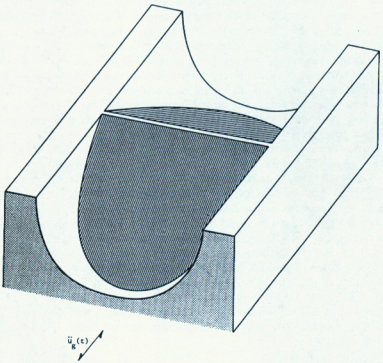

Figure 1. Three-dimensional view of dam in semi-cylindrical canyon

and participation factors for transient seismic excitation. Extensive comparisons are made with the results of 2-D plane-strain analyses of the dam mid-section, as well as with 3-D results for canyons of different shapes. It is worthy of note that the proposed method of analysis is at least three orders of magnitude less expensive than other presently available numerical procedures. A direct consequence: while not much information is presently available for the second and higher natural frequencies and mode shapes, or for the acceleration and strain transfer functions well beyond the fundamental frequency, such information is provided in this paper, which thereby offers new insights into the effects of valley geometry on the seismic response.

Although the choice of a semi-cylindrical (U-shaped) canyon was undoubtedly motivated by the ensuing mathematical convenience, such a shape does in fact constitute a reasonable idealization in many actual cases. For example, the valleys of the Kisenyama rockfill dam in Japan,[10] of El Infiernillo dam in Mexico[11] and of Rama earth dam in Yugoslavia,[12] just to name a few from the published literature, may be idealized with reasonable accuracy as semi-cylindrical.

SIMPLIFYING ASSUMPTIONS

With reference to Figure 2, the following simplifying assumptions are made in order to derive the governing equations of motion:

1. The dam consists of a uniform and linearly hysteretic continuum characterized by a constant mass density ρ, a constant shear modulus G and a constant hysteretic damping ratio β. The assumption of linear shear-stress–shear-strain behaviour is, of course, acceptable only for small levels of strain; it contradicts reality at shear strains larger than about 0·01 per cent. Note, however, that in practice this limitation may be approximately overcome by performing a series of linear analyses, each one using shear moduli and damping ratios consistent with the level of strains resulting from the previous analysis.[13,14] The assumption of a constant G, on the other hand, has been made for mathematical convenience, in the desire to achieve a closed-form analytical solution. In reality, for most soils G increases nearly in proportion to the square-root of the applied mean normal stress; hence, in earth dams, G increases with depth from the crest and away from the sloping faces, rather than remaining constant. Such an inhomogeneity may have an influence on the dynamic behaviour of an earth dam, as it is evident from the results of 2-D comparative studies.[15–18] However, results from a number of 3-D studies also suggest that the effects of inhomogeneity on the response are about the same for both 2-D and 3-D geometries.[4,8,19] Hence, a 3-D solution for a homogeneous dam, such as the one developed herein, can be extended to account approximately for material inhomogeneity.

2. The seismic excitation from the supporting semi-circular cylindrical valley involves exclusively horizontal motions in the upstream–downstream (lateral) direction. The vertical and longitudinal components of actual ground motions are ignored herein, since, as usual in earthquake engineering, their effects could be assessed independently from the effects of the lateral motion. No slippage is allowed at the dam–valley interface. Moreover, the supporting valley is assumed to vibrate as a rigid body, with all points at the dam–valley interface experiencing identical and synchronous (in-phase) oscillations; hence, a single accelerogram suffices to describe the excitation. Evidently, reality is more complicated. Seismic shaking is the result of a multitude of body and surface waves striking at various angles and creating reflection and diffraction phenomena; the resulting oscillations differ (in phase, amplitude and frequency characteristics) from point to point along the dam–valley interface. Nonetheless, the hypothesis of identical and synchronous excitation, advanced undoubtedly for mathematical convenience and employed invariably in all the aforementioned 3-D studies of earth dams, is a reasonable simplification for vertically incident plane SH-waves. For instance, the important wavelengths at frequencies f equal to, or near, the fundamental natural frequency f_1 of the dam are typically an order of magnitude larger than the dam height; hence, phase differences between arriving motions at point A and at point B (Figure 2) are small, i.e. the waves 'see' the dam almost as a mere point in space. However, this may not be true for the higher-frequency components of the motion. Trifunac[20] showed that, for wavelengths shorter than four times the radius of an infinitely-long earth-filled semi-cylindrical valley, substantial differences arise in both magnitude and phase angle of the motions at various points on the base.

3. Only horizontal lateral shear deformations take place with the attendant horizontal displacements, u, and shear stress, τ_{zy} and τ_{xy}, being independent of the y coordinate (uniformly distributed across the dam). These

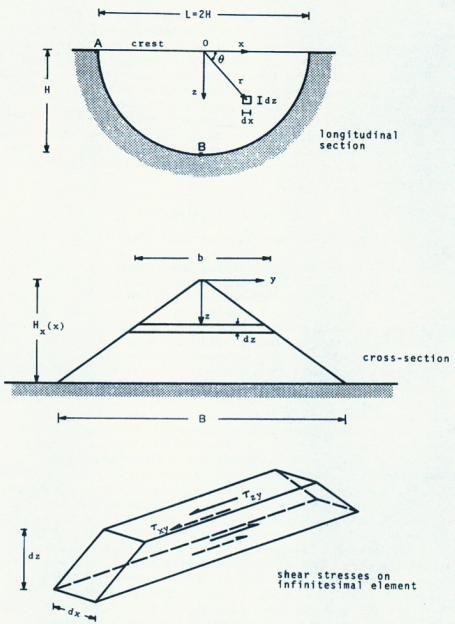

Figure 2. Longitudinal and lateral sections of dam; shear stresses acting on infinitesimal element

assumptions, previously introduced by Hatanaka[1] and Ambraseys,[2] constitute a reasonable simplification of the actual pattern of displacements and stresses. Thus, although vertical and longitudinal displacements do take place as a result of multiple wave reflections at the sloping faces and rock abutments, it is only the lateral horizontal displacements that are predominant in all but a few wave frequencies. Furthermore, in most cases, the actual distributions of shear stresses across the dam are indeed approximately uniform—the main

discrepancy arising from the unavoidable decline to zero of the actual stresses at the two (stress-free) sloping faces of the dam.[9, 15, 21, 22]

4. Hydrodynamic effects from the reservoir water are not taken into account. Recent studies on dam–water–soil interaction[23] confirm that for embankment dams such effects are, indeed, of only secondary importance.

FREE VIBRATION: ANALYSIS AND RESULTS

With the foregoing assumptions, consider the dynamic stresses acting on an infinitesimal horizontal element of the dam of volume $b\,dx\,dz = (B/H)\,z\,dx\,dz$ (Figure 2). The net shearing forces on the horizontal and vertical faces of this element are, respectively, expressed as

$$-\frac{B}{H}\frac{\partial}{\partial z}[z\,\tau_{zy}(x, z; t)]dx\,dz \tag{1a}$$

and

$$-\frac{B}{H}\frac{\partial}{\partial x}[\tau_{xy}(x, z; t)]z\,dx\,dz \tag{1b}$$

Denoting by $u = u(x, z; t)$ the lateral displacement *relative* to the boundaries, the total inertia force on the studied element equals

$$\rho\,\ddot{u}(x, z; t)\frac{B}{H}z\,dx\,dz \tag{1c}$$

with $\ddot{u} = \partial^2 u/\partial t^2$. Equating the sum of the above three forces to zero while accounting for the stress–displacement relations

$$\tau_{xy} = G\frac{\partial u}{\partial x},\ \tau_{zy} = G\frac{\partial u}{\partial z} \tag{2}$$

leads to the following equation of motion:

$$G\left(\frac{\partial^2 u}{\partial z^2} + \frac{\partial^2 u}{\partial x^2} + \frac{1}{z}\frac{\partial u}{\partial z}\right) = \rho\,\ddot{u} \tag{3}$$

To account for the dissipation of energy due to inelastic soil behaviour, linear hysteretic damping may be introduced in equation (3) by replacing G with the complex valued modulus $G^* = G(1 + 2i\beta)$, where β is the damping ratio and $i = \sqrt{-1}$. However, since the effect of damping on the natural frequencies and modal shapes is usually rather small, it is common practice to neglect it when analysing the free vibration characteristics of earth dams.[22] Instead, the damping ratio is introduced directly when studying forced vibrations, by superimposing properly damped modal responses. This practice is followed herein and, thus, the real shear modulus G is left in equation (3). The analysis with complex G^* is completely analogous, presenting no additional difficulty, as will be shown later.

In view of the shape of the boundary, it is computationally expedient to convert to polar cylindrical coordinates (Figure 2). After some algebra equation (3) transforms into

$$r^2\frac{\partial^2 u}{\partial r^2} + 2r\frac{\partial u}{\partial r} + \frac{\partial^2 u}{\partial \theta^2} + \cot\theta\frac{\partial u}{\partial \theta} = r^2\frac{\rho}{G}\ddot{u} \tag{4}$$

with $u = u(r, \theta; t)$. The solution of this equation must respect the free-vibration boundary conditions of vanishing displacements at the cylindrical base (no slippage, valley stationary):

$$u(H, \theta; t) = 0 \tag{5}$$

and of vanishing shear stresses at the crest:

$$G\frac{\partial u}{\partial z}(r, 0; t) = G\frac{\partial u}{\partial z}(r, \pi; t) = 0 \tag{6}$$

while u must attain a unique value, independent of θ at the centre of the crest:

$$\frac{\partial u}{\partial \theta}(0, \theta; t) = 0 \tag{7}$$

The steady-state solution of equation (4) may be cast in the form

$$u(r, \theta; t) = \Phi(r)\,\Psi(\theta)\exp(i\omega t) \tag{8}$$

Indeed, substitution into equation (4) yields

$$\frac{r^2}{\Phi(r)}\frac{\partial^2\Phi(r)}{\partial r^2} + \frac{2r}{\Phi(r)}\frac{\partial\Phi(r)}{\partial r} + k^2r^2 = -\frac{1}{\Psi(\theta)}\frac{\partial^2\Psi(\theta)}{\partial\theta^2} - \frac{\cot\theta}{\Psi(\theta)}\frac{\partial\Psi(\theta)}{\partial\theta} \tag{9}$$

in which $k = \omega/C_s$ (wave number) and $C_s = \sqrt{(G/\rho)}$ (wave velocity); ω represents circular frequency in rad/s. Since each side in equation (9) is an exclusive function of either r or θ, their equality is impossible unless they both attain a constant value, say a. Thus, two simultaneous independent equations are derived, one in $\Phi(r)$:

$$r^2\Phi'' + 2r\Phi' + (k^2r^2 - a)\Phi = 0 \tag{10}$$

and one in $\Psi(\theta)$:

$$\Psi'' + \cot\theta\,\Psi' + a\Psi = 0 \tag{11}$$

(The prime indicates derivative with respect to r or θ.)

Equation (10) is recognized as a Bessel equation. Its solution that is consistent with equation (6) reads

$$\Phi(r) = A'\frac{1}{r^{1/2}}J_v(kr) \tag{12}$$

$$v = (a + 1/4)^{1/2} \tag{13}$$

in which $J_v(\cdot)$ denotes the first-kind, v-order Bessel Function, and A' is an integration constant.

The solution to equation (11) is expressed in terms of two Gauss hyper-geometric functions* of a and $\cos^2\theta$:[24]

$$\Psi(\theta) = A''F\left(-\frac{\mu}{2}, \frac{\mu+1}{2}, \frac{1}{2}; \cos^2\theta\right) + A'''\cos\theta\,F\left(\frac{1-\mu}{2}, \frac{1+\mu}{2}, \frac{3}{2}; \cos^2\theta\right) \tag{14a}$$

with

$$\mu(\mu+1) = a \tag{14b}$$

Noticing that equations (7) and (8) require $\Psi(\theta)$ to be a constant, independent of θ, leads to $\mu = a = 0$, $A''' = 0$ and $\Psi(\theta) = A''$. Then, equation (13) simplifies to $v = 1/2$, the respective Bessel function can be expressed in terms of $\sin kr$, and by combining equations (8) and (12) the general solution is written as

$$u = A\left(\frac{2}{\pi k}\right)^{1/2}\frac{\sin kr}{r}\exp(i\omega t) \tag{15}$$

Enforcing equation (5) leads to $\sin kH = 0$, from which the natural circular frequencies ω_n (in rad/s) are readily recovered:

$$\omega_n = \pi n\frac{C_s}{H}; \quad n = 1, 2, 3, \ldots \tag{16a}$$

Alternatively, the natural frequencies f_n (in Hz) and periods T_n (in s) are

$$f_n = n\frac{C_s}{2H} \quad \text{and} \quad T_n = \frac{1}{n}\frac{2H}{C_s} \tag{16b}$$

---

* $F(\alpha, \beta, \gamma, x) = 1 + \sum_{k=1}^{\infty}\frac{\alpha(\alpha+1)\ldots(\alpha+k-1)\beta(\beta+1)\ldots(\beta+k-1)}{k!\,\gamma(\gamma+1)\ldots(\gamma+k-1)}x^k$

Substitution of equation (15) in equation (14) leads to the following modes of displacement amplitude, normalized to a unit maximum value at $r = 0$:

$$\bar{U}_n = \frac{\sin\left(n\pi\dfrac{r}{H}\right)}{n\pi\dfrac{r}{H}} \tag{17}$$

Results

As discussed in the introduction, it has been previously shown[1-7] that for earth dams built in relatively narrow valleys the plane-strain assumption utilized in the 2-D (and the shear-beam) response analyses may not be realistic. The rigid rock boundaries have a generally stiffening effect: natural frequencies increase and modal displacement shapes become sharper as the canyon becomes narrower.

The first of these phenomena is illustrated in Figure 3. In particular, Figure 3(a) shows the dependence of the fundamental natural frequency f_1 on the aspect ratio L/H and on the shape of the canyon. Four idealized shapes are studied, ranging from rectangle to triangle and including the semi-circle, for which $L/H = 2$ and $f_1 = 0{\cdot}50\, C_s/H$ [equation (16b)]. The fact that the latter expression plots very close to the fundamental frequency $f_1 \approx 0{\cdot}48\, C_s/H$ of a similar dam founded in a trapezoidal canyon with $L/H = 2$ and $L/B = 2^3$ is an indication of the accuracy of the developed solution. $f_{1,\mathrm{sb}} \approx 0{\cdot}38\, C_s/H$ represents the fundamental frequency of an infinitely long dam responding in pure shear.[1, 2, 22] The stiffening effect of the canyon geometry is evident in this figure. It should be noted, however, that other factors not explicitly recognized in Figure 3(a) may also have an effect on the computed fundamental frequency of a dam. Thus, the presence of a soft core leads to a lower first natural frequency, even when the average modulus remains the same.[10, 25] Also, whenever the analysis 'suppresses' one of the degrees of freedom of each point in the dam, the computed frequency (artificially) increases; this is the case with the shear beam as compared with the plane-strain analysis (vertical motion is suppressed in the former), and also with the analysis of Makdisi *et al.*[6] as compared with that of Mejia *et al.*[7, 8] (longitudinal motion is suppressed in the former). These remarks may help explain why the two 'data' points of Reference 8 (dam with core, 3-degrees-of-freedom per joint) plot quite lower than the lines computed from the results of Reference 6, for the same canyon geometry.

The higher natural frequencies f_n, $n = 2$–5, of dams in valleys with $L/H = 2$ are compared with the respective frequencies, $f_{n,\mathrm{sb}}$, of the infinitely long shear wedge in Figure 3(b). Results are available only for semi-cylindrical and rectangular canyons. Perhaps surprisingly, the differences among the three sets of frequencies wither away as n increases, and for $n \geqslant 3$ f_n appears to be practically independent of canyon geometry. However, this near-coincidence of higher natural frequencies is rather circumstantial and is due to the fact that the ratio f_n/f_1 for both of these canyons is lower than the corresponding $f_{n,\mathrm{sb}}/f_{1,\mathrm{sb}}$ ratio for the shear beam. For instance, equation (16b) for a dam in a semi-cylindrical canyon yields $f_3/f_1 = 3$, from which $f_3 = 1{\cdot}50\, C_s/H$; by contrast, the shear-beam solution gives $f_{3,\mathrm{sb}}/f_{1,\mathrm{sb}} \approx 8{\cdot}65/2{\cdot}41 \approx 3{\cdot}60$ from which $f_{3,\mathrm{sb}} \approx 3{\cdot}60 \times 0{\cdot}38\, C_s/H \approx 1{\cdot}37\, C_s/H$. Therefore, $f_{3,\mathrm{sb}}$ is only 8·7 per cent less than the 3-D value of f_3, compared with the 24 per cent discrepancy in the respective fundamental frequencies. It will be noted, however, in Figure 4 that the modal displacement shapes at these higher natural frequencies are at least as sensitive as the fundamental shape is to variations in canyon geometry.

The comparison of four natural mode shapes in Figure 4 also pertains to dams in a circular and a rectangular canyon (both with $L/H = 2$) and to the infinitely-long shear wedge. No published results are available to the authors for the mode shapes of dams in canyons of other shapes. Displacements normalized to a unit amplitude at mid-crest [Figure 4(a)] and shear strains γ_{xy} and γ_{zy} normalized to a unit amplitude at the base [Figure 4(b)] are considered. Shown are the distributions along the crest, $\bar{U}_n(x, z = 0)$ and $\bar{\Gamma}_{xy,n}(x, z = 0)$, and along the depth from mid-crest, $\bar{U}_n(x = 0, z)$ and $\bar{\Gamma}_{zy,n}(x = 0, z)$. These two distributions are identical in a cylindrical canyon, but differ from each other in a rectangular canyon. Notice that the cylindrical canyon leads to a sharper attenuation of displacements with depth from the crest, and to larger shear-strain values near the upper half of the dam.

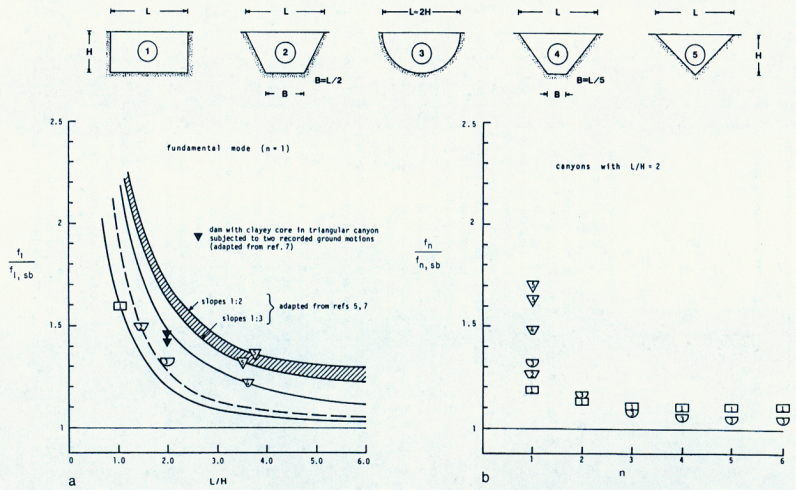

Figure 3. (a) Effect of canyon geometry on the fundamental natural frequency. (b) Effect of canyon shape on higher natural frequencies.

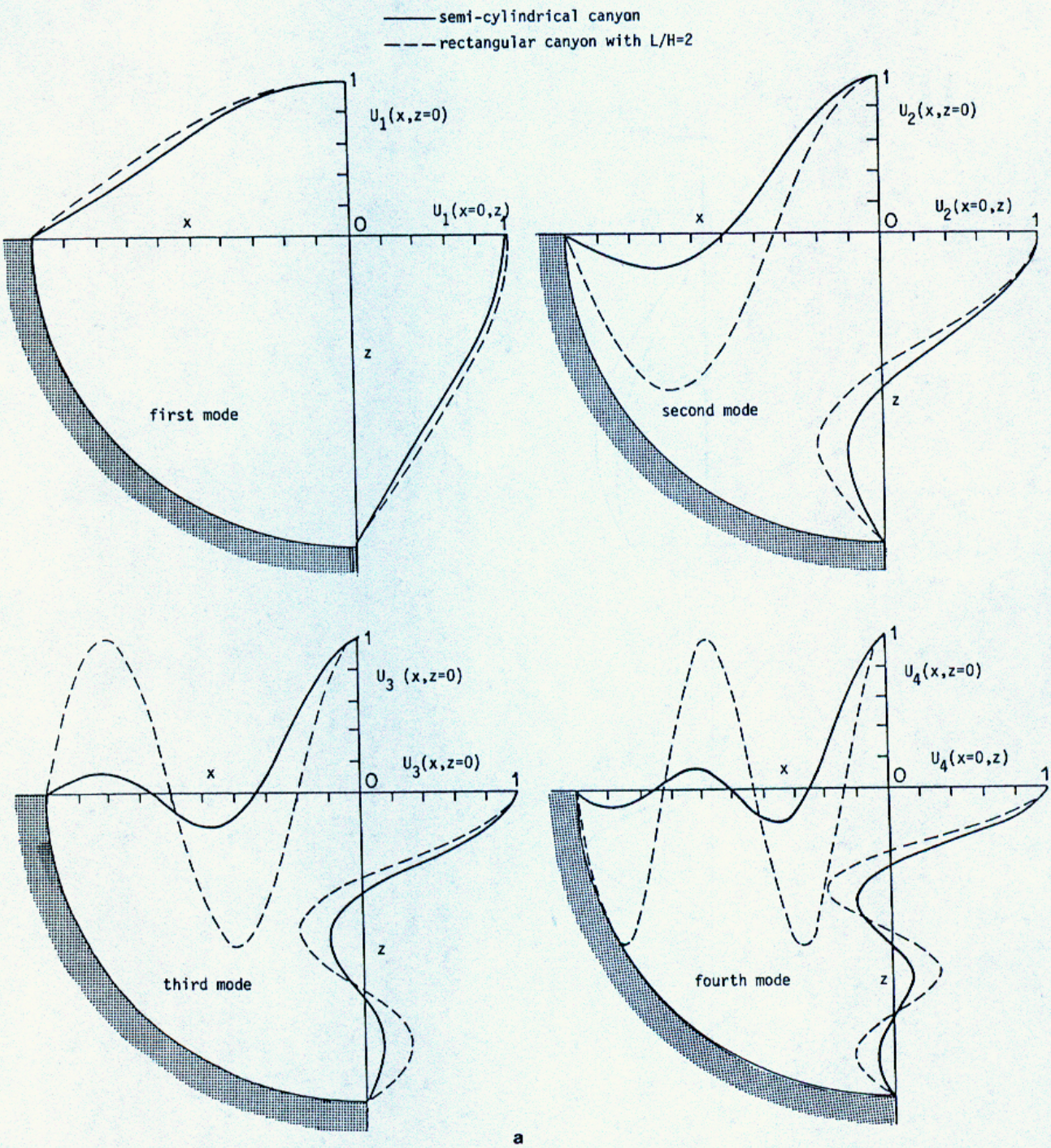

Figure 4. (a) Displacement and (b) shear-strain modal shapes for a semi-cylindrical and a rectangular canyon with $L/H = 2$

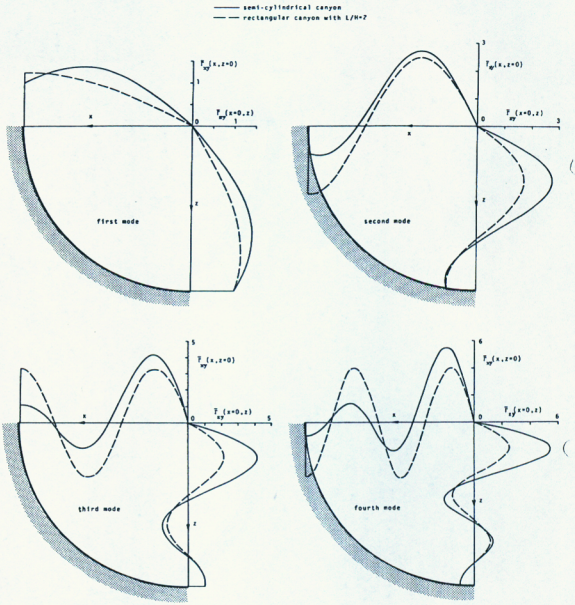
semi-cylindrical canyon
rectangular canyon with L/H=2
first mode
second mode
third mode
fourth mode

b

Figure 4(b).

RESPONSE TO BASE EXCITATION

When the valley is oscillating as a rigid base with an acceleration $\ddot{u}_g = \ddot{u}_g(t)$ in the y direction, the displacement $u = u(r, t)$ of the dam relative to the base is governed by

$$\frac{\partial^2 u}{\partial r^2} + 2r\frac{\partial u}{\partial r} = \frac{1}{C_s^2}(\ddot{u} + \ddot{u}_g) \tag{18}$$

For an arbitrary seismic base excitation $\ddot{u}_g(t)$, equation (18) is solved by mode superposition:*

$$u(r, t) = \sum_{n=1,2,\ldots}^{\infty} \bar{U}_n(r)\, P_n D_n(t) \tag{19}$$

in which $\bar{U}_n(r)$ is the nth mode displacement shape given in equation (17); P_n is the participation factor of the nth mode:

$$P_n = \frac{\int_0^H \int_0^{\pi} \bar{U}_n(r)\rho \dfrac{B}{H} r^2 \sin\theta \, d\theta \, dr}{\int_0^H \int_0^{\pi} \bar{U}_n^2(r)\rho \dfrac{B}{H} r^2 \sin\theta \, d\theta \, dr} = 2(-1)^{n+1} \tag{20}$$

and $D_n(t)$ is obtained by means of the Duhamel integral.[26]

From equation (19) expressions for the absolute acceleration $\ddot{u}_a$ and the maximum shear strain γ_{max} are directly recovered. For the former:

$$\ddot{u}_a(r, t) = \ddot{u}_g(t) + \sum_{n=1,2,\ldots}^{\infty} \bar{U}_n(r)\, P_n \ddot{D}_n(t) \tag{21}$$

For the latter, since evidently $\gamma_{r\theta} = \gamma_{\gamma\theta} = 0$ at every element,

$$\gamma_{max}(r, t) = \gamma_{rr}(r, t) = \sum_{n=1,2,\ldots}^{\infty} \frac{d\bar{U}_n(r)}{dr} P_n D_n(t) \tag{22}$$

When evaluating the series in equations (19) and (22) only the first few terms (usually not more than 3 or 4) need be considered. Convergence is slower, however, for the series associated with the absolute acceleration in equation (21).

Steady-state response

It is of interest to obtain the steady-state response to a harmonic base excitation $\ddot{u}_g(t) = \ddot{u}_g e^{i\omega t}$. In this case, equation (18) can be easily solved analytically for the relative lateral displacement $u(r; t) = u(r)e^{i\omega t}$:

$$\frac{u(r)}{u_g} = \frac{H}{r}\frac{\sin kr}{\sin kH} - 1 \tag{23}$$

from which the transfer function of the absolute acceleration, $\ddot{u} + \ddot{u}_g$, commonly called 'amplification' function, may be readily derived:

$$AF \equiv \frac{\ddot{u} + \ddot{u}_g}{\ddot{u}_g} = \frac{1}{\chi}\frac{\sin a_0\chi}{\sin a_0} \tag{24}$$

in which $\chi = r/H$ and $a_0 = \omega H/C_s$. Equations (23)–(24) are valid for both real C_s (material damping = 0) and complex $C_s^* = C_s\sqrt{(1 + 2i\beta)}$ (material hysteretic damping ratio = β); in the latter case use is made of the

* This is possible because the mode displacement shapes $\bar{U}_n(r)$ of equation (17) satisfy the 'orthogonality' condition: $I = \int_0^H \int_0^{\pi} \bar{U}_n(r)\bar{U}_m(r) dm(r, \theta) = 0$ if $n \neq m$; $dm(r, \theta)$ is the mass of an infinitesimal horizontal element. Indeed, in this case it can be shown the $I \propto \int_0^{\pi} \sin(n\pi p)\sin(m\pi p)\, dp$, which vanishes for $n \neq m$.

following expression for the sinus function of a complex number:

$$\sin(x+iy) = \sin x \cosh y + i \cos x \sinh y \tag{25}$$

Equation (24) is plotted in Figure 5 for three values of the depth parameter: $\chi = 0$ (mid-crest), 0·25 and 0·50. The results of a plane-strain shear-beam analysis for the mid-section of the dam are also shown for a comparison. It is evident that, in addition to predicting lower natural frequencies, the plane-strain model predicts lower values for the amplification at first and higher resonances.

The effects of canyon geometry on AF are illustrated through the comparison of Figure 6. All dams have an $L/H = 2$. Results for the triangular canyon (from Reference 6) are available for values of the frequency factor a_0 only up to about 5, and thus the comparison is limited to a frequency range encompassing only the fundamental and none of the higher frequencies of the studied dams. The curve for the rectangular canyon was prepared by the authors using the classical solution of Hatanaka[1] and Ambraseys.[2] The plots in Figure 6 exhibit a consistent trend and reveal that the value of AF at first resonance, AF_{max}, is practically independent of the exact canyon shape; for the considered value of the hysteretic damping ratio, $\beta = 0{\cdot}10$, $AF_{max} \approx 10$. Moreover, the results of Makdisi *et al.*[6] show that, in triangular valleys, $AF_{max} \approx 10$ for all values of the aspect ratio L/H!

Frequently in practical seismic analyses of dams built in narrow valleys, various cross-sections in addition to the mid-section are studied using plane-strain formulations. To investigate the validity of such a procedure, Figure 7 compares the plane-strain AF at the crest of the quarter-section ($x/L = 0{\cdot}25$) of a dam in a cylindrical valley, with the '3-D' AF computed from equation (24) for $r/H = 0{\cdot}50$. We notice that the plane-strain fundamental resonant peak exceeds the respective '3-D' resonant response by about 30 per cent. The discrepancies at higher frequencies are even greater, with the plane-strain solution always providing higher values than the developed ('3-D') model.

Also of great interest is the study of shear strains. Referring again to the mid-section of a dam in a cylindrical canyon, Figure 8 presents the variation with a_0 of the normalized steady-state shear-strain amplitude $\gamma_{xy}(r)C_s^2/(H\,\ddot{u}_g)$, for three depths $r = 0{\cdot}25H$, $0{\cdot}50H$ and H (bottom). Comparison with the corresponding plane-strain curves reveals a similar overall shape of the two sets of results, with the developed '3-D' solution invariably yielding lower peak resonant values; the difference reaches an appreciable 70 per cent at the base of the dam ($r/H = 1$).

The foregoing important conclusions are in full qualitative accord with the findings of Seed and his coworkers[6, 7] for dams in triangular canyons: the plane-strain solution for the mid-section provides lower values of accelerations but higher shear strains and stresses at the first resonance.

Seismic response

Earthquake ground excitation differs from a harmonic motion in two important aspects: it contains a fairly broad spectrum of frequencies, and it is of a random and transient nature. Thus, the seismic response will be transient and the effect of each 'contributing' frequency will not necessarily be the same as when the corresponding frequency component acts alone, under steady-state conditions.

As an example, the response of an idealized 120 m high dam in a U-shaped canyon is subjected to the N46W component of the ground acceleration recorded at the sub-basement of the 1901 Avenue of Stars building, in Los Angeles, during the 1971 San Fernando earthquake.[27] The time-history of acceleration scaled to a peak value of $0{\cdot}20g$, the Fourier amplitude spectrum, and the relative displacement and pseudo-acceleration response spectra for 5 and 10 per cent damping are presented in Figure 9. For this type of ground excitation, the dynamic uniform properties of the dam are taken: $C_s = 280$ m/s and $\beta = 10$ per cent.

The '3-D' acceleration, displacement and shear-strain response histories, computed with the presented theory for several points in the dam, are compared in Figures 10–12 with the respective histories computed for the dam mid-section by the shear-beam theory. The distributions with depth from the crest of the corresponding three sets of peak values are compared in Figure 13. The following trends are worthy of note in these figures.

1. The largest discrepancy between '3-D' and '2-D' (shear-beam) results is observed between the absolute acceleration histories; the '2-D' peak accelerations at the upper third of the dam are only about 40–50 per cent

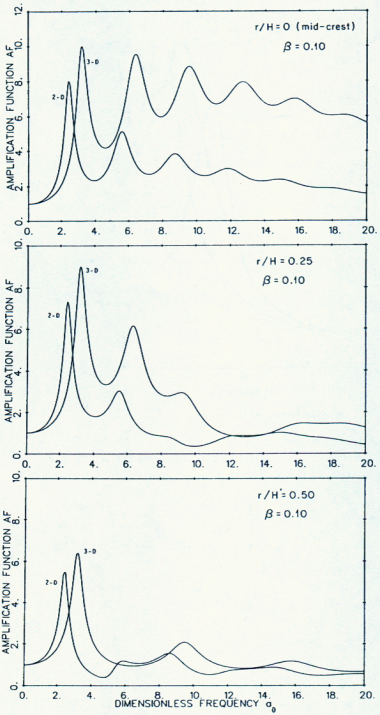

Figure 5. Steady-state response to harmonic base excitation: amplification functions at various depths in mid-section of semi-cylindrical dam determined from the developed theory ('3-D') and from plane-strain shear-beam analysis ('2-D')

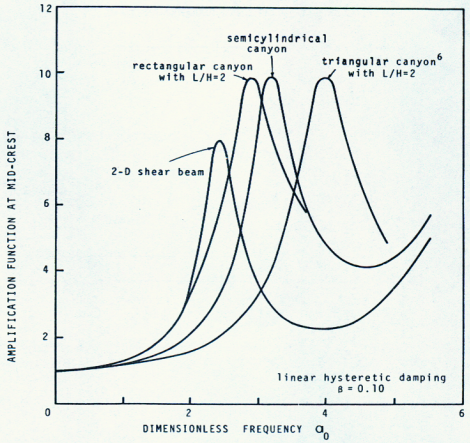

Figure 6. Effect of canyon shape on the mid-crest amplification function

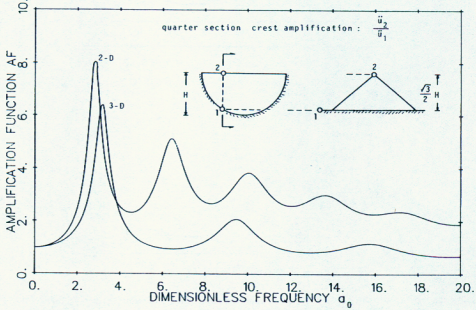

Figure 7. Crest amplification functions at the quarter section of semi-cylindrical dam from the developed theory ('3-D') and from plane-strain shear-beam analyses ('2-D')

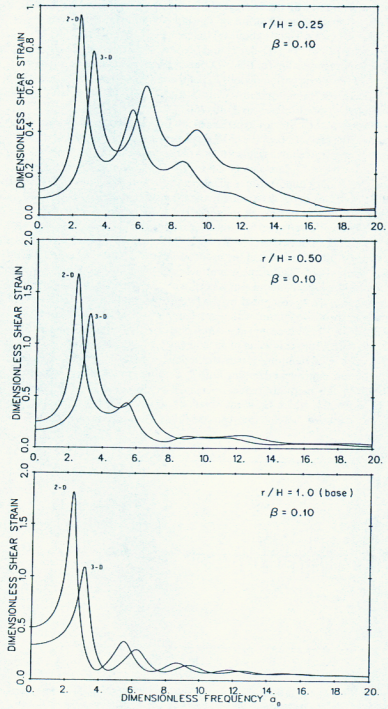

Figure 8. Shear-strain transfer functions at various depths in mid-section of semi-cylindrical dam determined from the developed theory ('3-D') and from plane-strain shear-beam analyses ('2-D') [Dimensionless shear strain = $\gamma_{rz}(r) \cdot C_s^2/(H\ddot{u}_g)$]

of the '3-D' values. This is consistent with the findings of Makdisi *et al.*,[6] and may be explained by noticing that: (i) the 10 per cent damped spectral acceleration of the input motion at the fundamental period $T_1 = 2 \times 120/280 \simeq 0{\cdot}86$ s of the '3-D' dam equals about $0{\cdot}11g$, compared to only $0{\cdot}09g$ which corresponds to $T_1 = T_{1,sb} \simeq 2{\cdot}61 \times 120/180 \simeq 1{\cdot}12$ s of the '2-D' dam;* and (ii) the contribution of the higher modes to the near-crest accelerations is much more important for the '3-D' dam, as evidenced in the comparison of Figure 5, and, also, by recalling that while the participation factor $|P_n|$ of the nth mode remains constant for the '3-D' dam [equation (20)], $|P_n|$ decreases monotonically with n for the '2-D' dam ($|P_1| \sim 1{\cdot}61$, $|P_2| \sim 1{\cdot}07$, $|P_3| \approx 0{\cdot}85$, $|P_4| \approx 0{\cdot}73$ and so on) (References 1, 10, 25).

2. By contrast, the displacement histories experienced by the two dams are very similar in magnitude, throughout the depth from the crest. In fact, the '2-D' displacements are higher by about 10 per cent. This is again explainable. First, the spectral relative displacements of the input motion at the two fundamental periods are equal to about 2·1 cm for the '3-D' dam and 2·8 cm for the '2-D' dam. And, second, as is well known, the higher modes are of only secondary importance to displacements. This is evident in Figure 11: oscillations of both '3-D' and '2-D' displacements occur at essentially the fundamental natural periods of each system (0·86 and 1·12 s, respectively), with smaller participation modes (i.e. lower periods). In fact, repeating the analyses which led to Figure 11 but with *only* the first mode participating in the response, yields very similar displacements histories; the peak values at the crest are apparently equal to 4·2 cm for the '3-D' dam and 4·5 cm for the '2-D' dam, which are within 25 per cent of the 'exact' values of 5·25 and 5·88 cm, respectively. Notice also the different frequency contents of displacement and acceleration histories; the latter exhibit vividly the substantial contribution by the higher modes—in accord with the remarks of the preceding paragraph.

3. The shear strains, $\gamma_{xy} = \gamma_{xy}(z; t)$, computed by the two analyses ('3-D' and '2-D') are of similar overall magnitude, differing only in their distribution with depth from the crest. The maximum peak value of γ_{xy} is in both cases slightly over 7×10^{-4}, but it occurs at a depth $z \approx H/3$ from the crest in the '3-D' analysis, while $z \approx 2H/3$ in the '2-D' analysis. From this value of γ_{xy} one may estimate an 'effective' shear strain amplitude $\gamma_e \approx 4 \times 10^{-4}$. Using experimental damping-versus-strain data (e.g. from Figure 8 of Reference 14), one can read for the above value of γ_e an equivalent damping ratio $\beta_e \approx 10$ per cent, which is equal to the value assumed in our analyses. Moreover, the modulus reduction-against-strain curve of Reference 14 yields for the equivalent modulus $G_e \approx 0{\cdot}50G_0$, where G_0 is the small strain ($\lesssim 10^{-6}$) shear modulus. Since an S-wave velocity of 280 m/s was assumed herein, one can postulate that an initial velocity of approximately

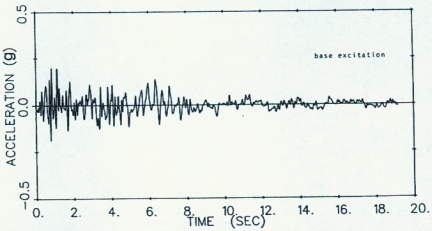

Figure 9. (a) Acceleration history recorded at sub-basement of 1901 Avenue of Stars, Los Angeles, in the 1971 San Fernando earthquake, scaled to a $0{\cdot}2g$ peak value (N46W Component).[27] (b) Corresponding Fourier amplitude and damped response spectra[27]

* Also notice the differences in the Fourier amplitudes at these periods.

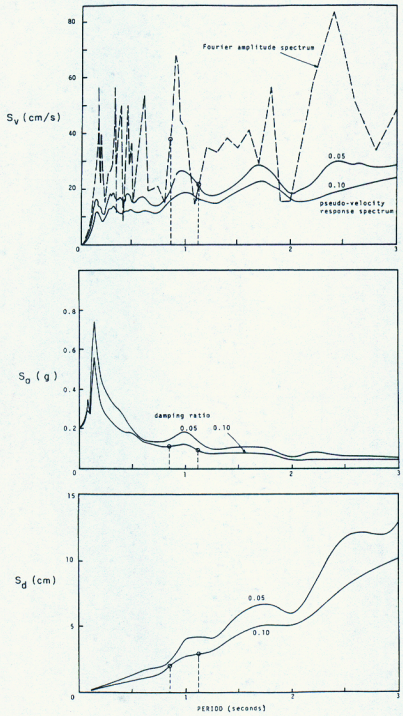
Fourier amplitude spectrum
S_v (cm/s)
0.05
0.10
pseudo-velocity response spectrum
S_a (g)
damping ratio
0.05
0.10
S_d (cm)
0.05
0.10
PERIOD (seconds)

Figure 9(b).

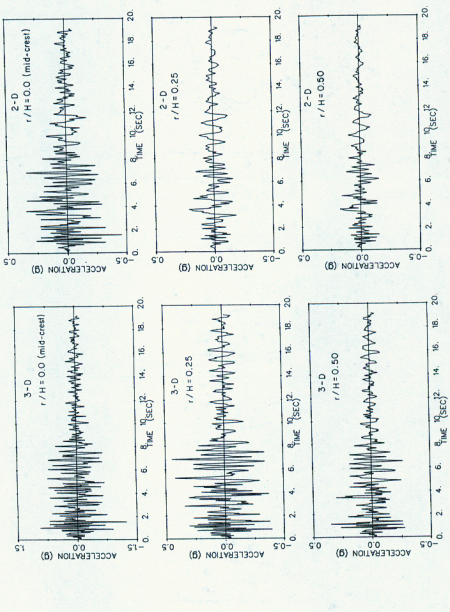

Figure 10. (a and b) Absolute acceleration response at various depths along the mid-section of a semi-cylindrical dam from the developed theory ('3-D') and from plane-strain shear-beam analyses ('2-D') (H = 120 m, C_s = 280 m/s and β = 0·10)

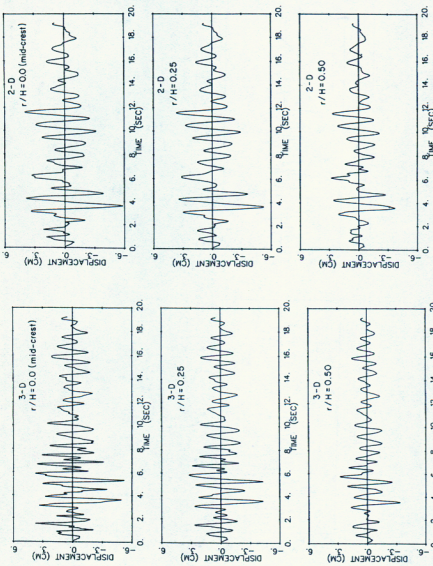

Figure 11. (a and b). Relative displacement response at various depths along the mid-section of a semi-cylindrical dam from the developed theory (3-D?) and from plane-strain linear beam analyses (2-D?) ($H = 120$ m, $c_s = 280$ m/s and $\beta = 0.10$)

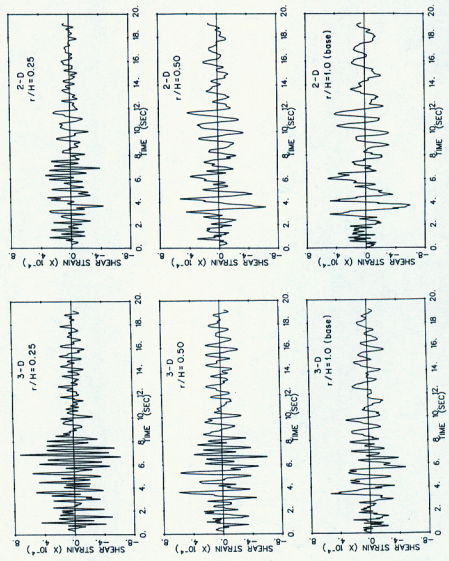

Figure 12. (a and b). Shear-strain γ_{xy} response at various depths along the mid-section of a semi-cylindrical dam from the developed theory ('3-D') and from plane-strain shear-beam analyses ('2-D') (H = 120 m, C_s = 280 m/s and β = 0·10)

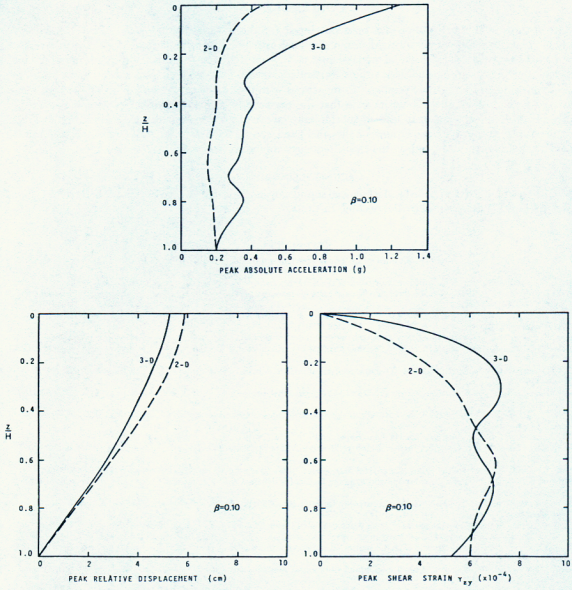

Figure 13. Distribution with depth of peak values of acceleration, displacement and shear strain γ_{xy} at mid-section of a semi-cylindrical dam from the developed theory ('3-D') and from plane-strain shear-beam analyses ('2-D') ($H = 120$ m, $C_s = 280$ m/s and $\beta = 0{\cdot}10$)

$280\sqrt{2} \approx 400$ m/s would be necessary to make the parameters used in the analyses *strain-compatible*. Indeed, 400 m/s is a realistic initial wave-velocity for a 120 m tall modern embankment dam.[8, 10, 11] Thus, the results and comparisons reported here are based on linear viscoelastic analyses which used moduli and damping ratios roughly consistent with the level of shear strain that would develop under moderately strong excitations in tall dams.

CONCLUSIONS

A closed-form analytical solution has been developed for the dynamic lateral linear shear response of embankment dams supported by rigid semi-cylindrical canyons. Extensive parameter studies have been conducted for natural frequencies and modal shapes, steady-state response to harmonic excitation, and seismic accelerations, displacements and shear strains. Particular emphasis has been given to assessing the importance of canyon geometry on seismic response. Comparisons with the results of '2-D' analyses of the dam mid-section (considered infinitely long) indicate that the presence of a semi-cylindrical canyon increases the fundamental frequency and may lead to substantially increased accelerations during earthquake shaking. Seismic displacements and shear strains, on the other hand, show a small sensitivity to canyon shape and their relative magnitudes will depend on the exact frequency content of the excitation.

ACKNOWLEDGEMENT

The authors gratefully acknowledge the financial support by the National Science Foundation, through Grant No. CEE–8205345 to Rensselaer Polytechnic Institute.

REFERENCES

1. M. Hatanaka, 'Fundamental considerations on earthquake resistant properties of the earth dam', *Disaster prevention res. inst. bull. Kyoto Univ.* No. 11 (1955).
2. N. N. Ambraseys, 'On the seismic behavior of earth dams', *Proc. 2nd world conf. earthquake eng.* Japan **1**, (1960).
3. B. Martinez and J. Bielak, 'On the three-dimensional seismic response of earth structures', *Proc. 7th world conf. earthquake eng.* Istanbul **8**, 523–528 (1980).
4. T. Ohmachi, 'Analysis of dynamic shear strain distributed in 3-dimensional earth dam models', *Proc. int. conf. recent advances geotech. earthquake eng. soil dyn.* St. Louis **1**, 459–464 (1981).
5. T. Ohmachi, 'Three-dimensional behavior of embankment dams', Presented at the *ASCE natl. convention exposition*, May (1981).
6. F. I. Makdisi, T. Kagawa and H. B. Seed, 'Seismic response of earth dams in triangular canyons', *J. geotech. eng. div. ASCE* **108**, 1328–1337 (1982).
7. L. H. Mejia, H. B. Seed and J. Lysmer, 'Dynamic analysis of earth dam in three dimensions', *J. geotech. eng. div. ASCE* **108**, 1586–1604 (1982).
8. L. H. Mejia and H. B. Seed, 'Comparison of 2-D and 3-D dynamic analyses of earth dams', *J. geotech. eng. div. ASCE* **109**, 1383–1398 (1983).
9. A. M. Abdel-Ghaffar and A. S. Koh, 'Three-dimensional dynamic analysis of nonhomogeneous earth dams', *Soil dyn. earthquake eng.* **1**, 136–144 (1982).
10. S. Okamoto, *Introduction to Earthquake Engineering*, 2nd edn., University of Tokyo Press, 1984.
11. D. Resendiz, M. P. Romo and E. Moreno, 'El Infiernillo and LaVillita dams: seismic behavior', *J. geotech. eng. div. ASCE* **108**, 109–131 (1982).
12. T. Paskalov, 'Comparative analysis of a rockfill dam', *Proc. 7th world conf. earthquake eng.* Istanbul **8**, 125–132 (1980).
13. H. B. Seed and I. M. Idriss, 'Soil moduli and damping factors for dynamic response analyses', University of California Berkeley *Research Report EERC 70-10* 1970.
14. F. I. Makdisi and H. B. Seed, 'Simplified procedure for estimating dam and embankment earthquake-induced deformations', *J. geotech. eng. div. ASCE* **104**, 849–867, (1978).
15. G. Gazetas, 'A new dynamic model for earth dams evaluated through case histories', *Soils found.* **21**, 67–68 (1981).
16. G. Gazetas, 'Shear vibrations of vertically inhomogeneous earth dams', *Int. j. numer. anal. methods geomech.* **6**, 219–241 (1982).
17. G. Gazetas, A. Debchaudhury and D. A. Gasparini, 'Random vibration analysis of earth dam seismic response', *Geotechnique*, **31**, 261–279 (1981).
18. A. M. Abdel-Ghaffar and A. S. Koh, 'Longitudinal vibration of nonhomogeneous earth dams', *Earthquake eng. struct. dyn.*, 9, 3, 279–305 (1981).
19. M. Oner, 'Shear vibration of inhomogeneous earth dams in rectangular canyons', *Soil dyn. earthquake eng.* **3**, 19–26 (1984).
20. M. D. Trifunac, 'Scattering of plane SH waves by a semi-cylindrical canyon', *Earthquake eng. struct. dyn.* **1**, 267–281 (1973).
21. A. K. Chopra, M. Dibaj, R. W. Clough, J. Penzien and H. B. Seed, 'Earthquake analysis of earth dams', *Proc. 4th world conf. earthquake eng.* Santiago, Chile **A-5**, 55–72 (1969).
22. H. B. Seed and G. R. Martin, 'The seismic coefficient in earth dam design', *J. soil mech. found. div. ASCE* **92**, No. SM3, 25–58 (1966).
23. J. F. Hall and A. K. Chopra, 'Hydrodynamic effects in earthquake response of embankment dams', *J. geotech. eng. div. ASCE* **108**, 591–598 (1982).
24. E. Kamke, *Differentialgleichungen Losungsmethoden und Losungen*, Chelsea Publ. Co., New York, 1959.
25. G. Tsiatas and G. Gazetas, 'Plane-strain and shear beam free vibration of earth dams', *Soil dyn. earthquake eng.* **1**, 150–160 (1982).
26. R. W. Clough and J. Penzien, *Dynamics of Structures*, Wiley, New York, 1975.
27. California Institute of Technology, 'Strong motion earthquake accelerograms', *Report No. EERL 71-50*, 1970.